Two-pion exchange NN potential from Lorentz-invariant χEFT*

R. Higa[a†], M.R. Robilotta[b], C.A. da Rocha[c]

[a]Jefferson Laboratory, 12000 Jefferson Avenue MS12H2, Newport News, VA 23606, USA

[b]Physics Institute, University of São Paulo, C.P. 66318, 05315-970, São Paulo, SP, Brazil

[c]Núcleo de Pesquisa em Bioengenharia, Universidade São Judas Tadeu, Rua Taquari, 546, 03166-000, São Paulo, SP, Brazil

We outline the progress made in the past five years by the São Paulo group in the development of a two-pion exchange nucleon-nucleon potential within a Lorentz-invariant framework of (baryon) chiral perturbation theory.

1. Motivation: the problem in the heavy baryon formalism

In the works of Becher and Leutwyler [1] it was shown that the convergence of the chiral expansion of the nucleon scalar form factor, driven by the triangle diagram of Fig. 1, is a delicate issue for values of the momentum transfer t near $(2m_\pi)^2$ due to the presence of an anomalous threshold, *i.e.* a branch point in the second Riemann sheet right below the two-pion threshold. Such a singularity is completely neglected in heavy baryon chiral perturbation theory (HBχPT), and can only be recovered by resumming the heavy baryon series to all orders. In order to understand this problem one can start from the spectral representation of the triangle integral,

$$\gamma(t) = \frac{1}{\pi}\int_{4m_\pi^2}^{\infty}\frac{dt'}{(t'-t)}\,\mathrm{Im}\gamma(t')\,, \quad \text{where} \quad \mathrm{Im}\gamma(t') \simeq \frac{\theta(t'-4m_\pi^2)}{16\pi m_N\sqrt{t'}}\,\arctan\frac{2m_N\sqrt{t'-4m_\pi^2}}{t'-2m_\pi^2}\,. \quad (1)$$

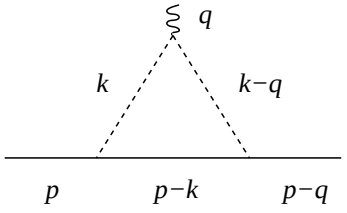

Figure 1. The triangle diagram that contributes to the nucleon scalar form factor. The solid, dashed, and wiggly lines represent, respectively, the nucleon, the pions, and an external scalar-isoscalar source.

*Notice: Authored by Jefferson Science Associates, LLC under U.S. DOE Contract No. DE-AC05-06OR23177. The U.S. Government retains a non-exclusive, paid-up, irrevocable, world-wide license to publish or reproduce this manuscript for U.S. Government purposes.

†Present address: Helmholtz-Institut für Strahlen- und Kernphysik, Universität Bonn, Nußallee 14-16, Bonn, Germany, 53115. Email: higa@itkp.uni-bonn.de.

Formally, the argument $x = 2m_N\sqrt{t'-4m_\pi^2}/(t'-2m_\pi^2)$ is counted as order q^{-1} and the HB expansion yields $\tan^{-1} x = \pi/2 - 1/x + 1/3x^3 + \cdots$, but this is valid only in the domain $|x| \geq 1$. The first two terms reproduce the HB result for the triangle graph,

$$\begin{aligned}\gamma(-q^2)|_{HB} &= \frac{1}{16\pi^2 m_N m_\pi}\int_{4m_\pi^2}^{\infty}\frac{dt'}{(t'+q^2)}\,\frac{1}{\sqrt{t'}}\left[\frac{\pi}{2}-\frac{(t'-2m_\pi^2)}{2m_N\sqrt{t'-4m_\pi^2}}\right] \\ &= \frac{1}{16\pi^2 m_N m_\pi}\left[2\pi m_\pi\, A(q)+\frac{m_\pi}{m_N}\,\frac{(2m_\pi^2+q^2)}{(4m_\pi^2+q^2)}\,L(q)\right], \qquad (2)\end{aligned}$$

where $q = |\boldsymbol{q}|$, and $L(q)$ and $A(q)$ are the usual HB loop functions,

$$L(q) = \frac{\sqrt{4m_\pi^2+q^2}}{q}\,\ln\frac{\sqrt{4m_\pi^2+q^2}+q}{2m_\pi}, \qquad A(q) = \frac{1}{2q}\,\arctan\frac{q}{2m_\pi}. \qquad (3)$$

However, it does not take into consideration the case $|x| < 1$, where t' gets closer to $4m_\pi^2$. This region determines the long distance behavior of the triangle diagram, as can be seen by its representation in configuration space [2],

$$\Gamma(r) = \frac{1}{\pi}\int_{4m_\pi^2}^{\infty} dt' \int \frac{d^3q}{(2\pi)^3}\, e^{-i\boldsymbol{q}\cdot\boldsymbol{r}}\,\frac{\mathrm{Im}\gamma(t')}{t'+q^2} = \frac{1}{4\pi^2}\int_{4m_\pi^2}^{\infty} dt'\,\frac{e^{-r\sqrt{t'}}}{r}\,\mathrm{Im}\gamma(t'). \qquad (4)$$

Clearly one sees that, in order to have a good asymptotic description of $\Gamma(r)$, one needs a decent representation for $\mathrm{Im}\gamma(t')$ near $t' = 4m_\pi^2$, which cannot be provided by HBχPT.

We want to stress that the expansion in $1/m_N$ of our two-pion exchange nucleon-nucleon potential (TPEP) should, in principle, recover the expressions from HBχPT, and we used this fact as a cross-checking of our calculation (see next section). However one must keep in mind that, due to the problem described above, such an expansion should not be done.

2. Comparison of HB- and RB-χPT results

The technical details in the evaluation of our TPEP is described in Refs. [2,3,4]. Our loop integrals are calculated relativistically using dimensional regularization in the $\overline{\mathrm{MS}}$ scheme, and we showed that they become almost identical as the infrared-regularized results in configuration space for distances above 1fm [3]. Because we are constructing the kernel of the interaction in a relativistic way one has to deal with the subtraction of the iterated one-pion exchange, with the intermediate two-nucleon propagating only with positive energy. The subtraction of this contribution is not unique, and in [2,3] we adopted the Blankenbecler-Sugar prescription.

The $1/m_N$ expansion of our TPEP and comparison with the HB results were shown in [2], where we initially found 14 different terms out of lengthy expressions, which will not be reproduced here. We revised our calculations, in particular the two loop contributions [4,5], and with the corrected expressions these differences dropped down to 9 terms. Their origins are now better understood: six of them come from the prescription for the subtraction of the iterated one-pion exchange, and using the same procedure of Ref. [6]

(see [4]) those differences went away. The remaining three come from two loop diagrams, and the reason for such a discrepancy is harder to access. It is quite possible that they come from the way the one-loop counterterms in the πN amplitude were renormalized [7,5]. Numerically they are not significant [4], but if one aims at increasing precision this technical issue may have to be revisited.

From now on we will ignore these differences and focus only on the effect of the $1/m_N$ expansion. To regularize the short-distance divergence one considers a phenomenological cutoff of the Argonne V14-V18 type,

$$[1 - \exp(-cr^2)]^4 \,, \tag{5}$$

with $c = 2\text{fm}^{-2}$, and in the remaining of this section one adopts the πN LECs from Entem and Machleidt [8] (to be discussed in the next section). The NN potential is further supplemented with the usual charge-dependent one-pion exchange.

Figs. 2 and 3 show the ratios of the $1/m_N$ expanded (HB) over the non-expanded (RB) TPE potentials for ${}^3F_2$ and ${}^1F_3$ partial waves and they represent, respectively, what one observes for the total isospin $T = 1$ and $T = 0$ channels. For $T = 1$ waves the ratio follows the behavior of the loop integrals [3], with differences of $\sim 20\%$ at $r = 10$fm and increasing with the distance. On the other hand, the $T = 0$ case shows a sizeable factor of 1.7 already at $r \sim 6$fm. A numerical investigation suggests that a significant cancellation happens between the isoscalar and isovector components in this region [4], therefore amplifying the difference between the HB and RB results.

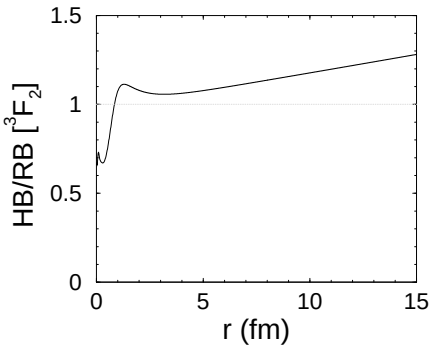

Figure 2. ${}^3F_2$ partial wave projection of the ratio HB- over the RB-χPT TPEP.

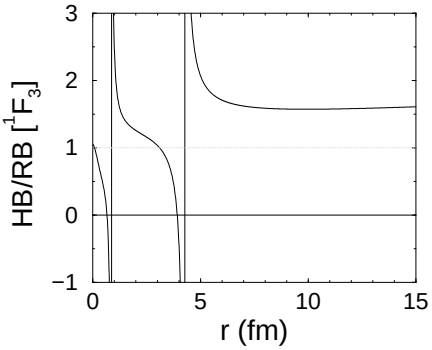

Figure 3. ${}^1F_3$ partial wave projection of the ratio HB- over the RB-χPT TPEP.

3. LECs and phase shifts

Table 1 shows the values of the πN LECs considered in Ref. [4], and there you can also find a short description on the extraction of each related work. The important observation to be made is the large spread in the central value of these constants, usually extracted from πN scattering with large uncertainties, and the question to ask is whether peripheral NN scattering is able to restrict some of these sets of LECs.

Table 1
Values for the πN LECs from the $O(q^2)$ Lagrangian, used in Ref. [4].

LEC	EM [8]	Mojžiš [9]	BM [10]	FMS (fit 1) [11]	Nijmegen [12]
c_1	-0.81	-0.94	-0.81	-1.23	-0.76
c_2	3.28	3.20	8.43	3.28	3.20
c_3	-3.40	-5.40	-4.70	-5.94	-4.78
c_4	3.40	3.47	3.40	3.47	3.96

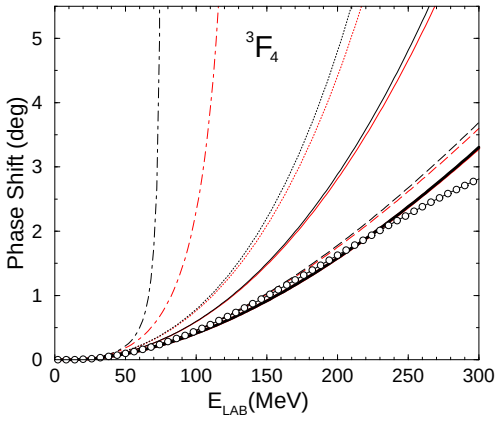

Figure 4. $^3F_4$ phase shift predictions using the LECs in table 1. Solid, thick line: Entem and Machleidt [8], dotted: Mojžiš [9], dashed: Büttiker and Meißner [10], dot-dashed: Fettes *et.al.* [11], solid, thinner line: Nijmegen [12]. The light and dark curves correspond to the HB and RB expressions, respectively, and the circled line, to the Nijmegen partial wave analysis [13].

In Fig. 4 we show the $^3F_4$ phase shifts for the LECs in table 1. Despite from what one sees in Figs. 2 and 3, the difference between HB and RB predictions for phase shifts is quite small, except for values of LECs from Fettes *et.al.* and Mojžiš, which are not consistent with Nijmegen's partial wave analysis [13] (PWA) anyway. The reason is that the potentials differ significantly after $r \sim 5$fm, where the TPEP is already too small and gets washed away by the OPEP.

Concerning the LECs, our results show more sensitivity to the constant c_3, which controls the strength of the attractive, central scalar-isoscalar potential. It can be inferred from the values of Fettes *et.al.* and Mojžiš (and a bit less from Nijmegen), which have larger values for $|c_3|$ and produces larger, positive contributions to the phase shifts. We also varied the cutoff parameter c in Eq. 5 between 1.5 and 2.5 fm^{-2} and observed very small variations and good overall agreement with PWA using the LECs from Entem and Machleidt, and slightly bigger variations and disagreement in some waves for values from Büttiker and Meißner. In the case of Nijmegen, agreement with PWA is possible in some waves only with a cutoff as low as 1.0fm^{-2}, and keeping this as a lower limit for c, no agreement with PWA is reached for LECs from Fettes *et.al.* or from Mojžiš. This indicates that peripheral nucleon-nucleon scattering favors smaller absolute values for the LEC c_3.

A question that arises is why the LECs extracted by the Nijmegen group, from the nucleon-nucleon scattering data, does not seem to be compatible with their own PWA. Part of the answer comes from the fact that in Refs. [4,8] the expressions for the $O(q^4)$ NN potential were used, while in the Nijmegen work, the $O(q^3)$ NN potential was employed. This fact is illustrated in Fig. 5, where in the dashed, light curve the Nijmegen values for

the LECs were used on the $O(q^3)$ expressions for the NN potential. Another possible contribution to this discrepancy could be the fact that we are solving the usual Schrödinger equation, while the Nijmegen group employs the relativistic Schrödinger equation in their analysis. This may account for the remaining discrepancy and is a topic yet to be investigated.

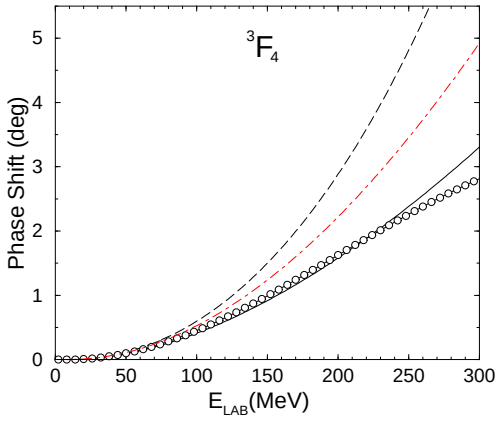

Figure 5. $^3F_4$ phase shift results for the $O(q^4)$ chiral potential with LECs from Entem and Machleidt [8] (solid curve), $O(q^3)$ (dashed, light curve) and $O(q^4)$ (dashed, dark curve) chiral potential with LECs from the Nijmegen group [12], and comparison with Nijmegen partial wave analysis [13] (circles).

4. Acknowledgements

R. H. would like to thank the organizers of the 18th International IUPAP Conference on Few-Body Problems in Physics for the excellent conference and opportunity to present this talk.

REFERENCES

1. T. Becher and H. Leutwyler, Eur. Phys. Journal C **9**, 643 (1999); JHEP **106**, 17 (2001).
2. R. Higa and M.R. Robilotta, Phys. Rev. C **68**, 024004 (2003).
3. R. Higa, M. R. Robilotta, and C. A. da Rocha, Phys. Rev. C **69**, 034009 (2004).
4. R. Higa, arXiv: nucl-th/0411046.
5. R. Higa, M. R. Robilotta, and C. A. da Rocha, in preparation.
6. N. Kaiser, R. Brockman, and W. Weise, Nucl. Phys. **A625**, 758 (1997).
7. N. Kaiser, Phys. Rev. C **64**, 057001 (2001).
8. D. R. Entem and R. Machleidt, Phys. Rev. C **66**, 014002 (2002).
9. M. Mojžiš, Eur. Phys. J. **C 2**, 181 (1998).
10. P. Büttiker and U.-G. Meißner, Nucl. Phys. **A668**, 97 (2000).
11. N. Fettes, U.-G. Meißner, and S. Steininger, Nucl. Phys. **A640**, 199 (1998).
12. M. C. M. Rentmeester, R. G. E. Timmermans, and J. J. de Swart, Phys. Rev. C **67**, 044001 (2003).
13. Nijmegen on-line program, http://nn-online.org.